


 Cite this: *CrystEngComm*, 2014, 16, 10006

Structures and properties of coordination polymers involving asymmetric biphenyl-3,2',5'-tricarboxylate†

 Jie Zhao,^a Li-Qiong Xie,^a Ying-Ming Ma,^a Ai-Ju Zhou,^a Wen Dong,^a Jing Wang,^{*a} Yan-Cong Chen^b and Ming-Liang Tong^b

An asymmetric polycarboxylate ligand, biphenyl-3,2',5'-tricarboxylic acid (H₃bptc) with a rotatable coordination vertex, was employed to react with metal ions under hydrothermal conditions. Four new coordination polymers {[Mn₃(bptc)₂(4,4'-bpy)₃(H₂O)₂]_n} (1), {[Ni(Hbptc)(4,4'-bpy)_{1.5}(H₂O)₂·H₂O]_n} (2), {[Cd₂(Hbptc)₂(phen)₄·3H₂O]_n} (3) and {[Cu₂(Hbptc)₂(2,2'-bpy)₂(H₂O)₂·2H₂O]_n} (4) were successfully synthesized and characterized. Single crystal X-ray analysis revealed that compound 1 has a 3D coordination network with linear Mn(II)-based subunits, while 2 is a 1D ladder chain-based structure further interconnected by hydrogen bonds to a 3D supramolecular network. Compounds 3 and 4 are each composed of a supramolecular network, which is supported by hydrogen bonds and π···π interactions and consists of dimers, [Cd₂(Hbptc)₂(phen)₄] and [Cu₂(Hbptc)₂(2,2'-bpy)₂], respectively. The conformation stability and coordination modes of the H₃bptc ligand have been discussed. The magnetic and fluorescent properties of the complexes have been investigated.

 Received 15th June 2014,
Accepted 28th August 2014

DOI: 10.1039/c4ce01225a

www.rsc.org/crystengcomm

Introduction

In the field of materials science, much research has been conducted on coordination polymers, based on metal centres and multifunctional bridging ligands, due to their fascinating structures and new topologies, as well as their tremendous potential applications as functional materials including catalysis, gas storage, fluorescent sensing, electronic and magnetic devices.¹ More and more efforts have mainly been focused on the construction and preparation of versatile coordination polymers and their structure–property relationships. The structural information stored in the organic ligands along with the coordination geometry of the metal ions should be taken into account. Therefore, the judicious choice and design of organic moieties is very important for constructing novel structures, and searching new bridging ligands is of great

interest and challenge.² Many construction features of ligands could affect the structural assembly process of these materials, such as their size and shape, the flexibility and the functional groups within the ligands.³

Polycarboxylate ligands have been proven to be good candidates for constructing novel structures, because they can be regarded not only as hydrogen bond acceptors but also as donors, depending on the number of deprotonated carboxylic groups. Of the aromatic carboxylates, the rigid 1,4-benzenedicarboxylate,⁴ 1,3,5-benzenetricarboxylate,⁵ 1,2,4,5-benzenetetracarboxylate,⁶ 1,2,3,4,5-benzenepentacarboxylate⁷ and 1,2,3,4,5,6-benzenehexacarboxylate⁸ were studied extensively to construct numerous coordination polymers. Compared to those rigid aromatic ligands, semi-rigid biphenyl ligands possess more flexibility, because of the free rotation around the C–C bond between the phenyl rings, and therefore may build coordination polymers with more diverse structures. More recently, versatile coordination polymers, assembled from biphenyl carboxylate ligands, such as biphenyldicarboxylate,⁹ biphenyl-3,4',5-tricarboxylate,¹⁰ and biphenyl-3,5,3',5'/3,4,3',4'/2,4,2',4'-tetracarboxylate¹¹ compounds, have been reported. Most of these polycarboxylate ligands possess a highly symmetric geometry which results in symmetric networks. In contrast, coordination polymers based on asymmetric polycarboxylate ligands are far less prevalent, probably due to their asymmetric geometry, making it difficult to predict and control the final coordination networks.¹²

^a Guangzhou Key Laboratory for Environmentally Functional Materials and Technology, School of Chemistry and Chemical Engineering, Guangzhou University, Guangzhou 510006, PR China. E-mail: wangjgzhu@163.com; Fax: +86-02039366908; Tel: +86-02039366908

^b State Key Laboratory of Optoelectronic Materials and Technologies, School of Chemistry and Chemical Engineering, Sun Yat-Sen University, Guangzhou 510275, PR China

† Electronic supplementary information (ESI) available: Crystallographic data in CIF format for 1–4, computational details for free H₃bptc, XRPD patterns for 1–4, TG curves for 1–4, excitation and emission spectra for 1, 2 and 4, selected bond lengths and angles for 1–4, hydrogen bond lengths and angles for 2 and 4. CCDC 996435–996438. For ESI and crystallographic data in CIF or other electronic format see DOI: 10.1039/c4ce01225a

To the best of our knowledge, coordination polymers based on biphenyl-3,2',5'-tricarboxylic acid (H_3bptc) have been rarely documented.¹³ H_3bptc , as one type of bridging biphenyl polycarboxylate ligand, has a rotatable coordination vertex and an asymmetric geometry with three carboxylate groups. Learning from our previous study on conformational flexible cyclohexane-polycarboxylate coordination polymers,¹⁴ the H_3bptc with a rotatable coordination vertex and asymmetric geometry may be a good candidate for constructing versatile coordination networks with functional properties. With the introduction of an auxiliary ligand, such as 4,4'-bipyridine (4,4'-bpy), 1,10-phenanthroline (phen) and 2,2'-bipyridine (2,2'-bpy) into the reaction system, four new coordination polymers have been obtained. Herein, we report the syntheses and structural characterizations of the four new coordination polymers, $\{[Mn_3(bptc)_2(4,4'-bpy)_3(H_2O)_2]\}_n$ (1), $\{[Ni(Hbptc)(4,4'-bpy)_{1.5}(H_2O)_2]\cdot H_2O\}_n$ (2), $\{[Cd_2(Hbptc)_2(phen)_4]\cdot 3H_2O\}_n$ (3), $\{[Cu_2(Hbptc)_2(2,2'-bpy)_2(H_2O)_2]\cdot 2H_2O\}_n$ (4), which exhibit a systematic variation of architectures from an 0D dimer to a 3D framework constructed from deprotonated H_3bptc and the auxiliary ligands. The conformation stability and coordination modes of the H_3bptc ligand have been discussed. In addition, the magnetic and fluorescent properties of the complexes have been investigated.

Experimental section

Materials and methods

The reagents and solvents employed were commercially available and used as received without further purification. The C, H, and N microanalyses for the four compounds were performed with fresh samples using an Elementar Vario-EL CHN elemental analyzer. FT-IR spectra were recorded with KBr pellets in the range of 4000–400 cm^{-1} using a Bio-Rad FTS-7 spectrometer. X-ray powder diffraction (XRPD) intensities for the four compounds were measured at 293 K using a Bruker D8 X-ray diffractometer (Cu-K α , $\lambda = 1.54056 \text{ \AA}$). The crushed poly-crystalline powder samples were prepared by crushing the crystals and scanned from 5–60° with a step rate of 0.1° s^{-1} , and the calculated patterns were generated with PowderCell. Thermogravimetric (TG) analyses were carried out using the NETZSCH TG209F3 thermogravimetric analyzer. Variable-temperature magnetic susceptibility measurements were performed using a SQUID magnetometer MPMS (Quantum Design) at 1.0 kOe for 1, 2, 4, and the diamagnetic correction was applied using Pascal's constants. The emission/excitation spectra for 1–4 were measured using an F-4500 Fluorescence Spectrophotometer.

Synthesis of $\{[Mn_3(bptc)_2(4,4'-bpy)_3(H_2O)_2]\}_n$ (1). A mixture of H_3bptc (0.053 g, 0.20 mmol) and 4,4'-bpy (0.156 g, 1.00 mmol) in H_2O (5.0 mL) was added to an aqueous solution (12.0 mL) of $Mn(OAc)_2\cdot 4H_2O$ (0.123 g, 0.50 mmol) and stirred. The resultant solution was heated in a stainless steel reactor with Teflon liner at 120 °C for 120 h. After a period of approximately 12 h cooling to room temperature, colorless block crystals of 1 (yield *ca.* 78% based on Mn) were obtained, isolated by filtration and washed

with water. IR (KBr, cm^{-1}): 3626w, 3072w, 2367w, 1582s, 1385s, 1224w, 1073w, 819m, 784m, 714w, 645m, 518w. Elemental analysis calcd for $C_{30}H_{21}N_3O_7Mn_{1.50}$: C, 58.31; H, 3.43; N, 6.80. Found: C, 58.99; H, 3.10; N, 6.95.

Synthesis of $\{[Ni(Hbptc)(4,4'-bpy)_{1.5}(H_2O)_2]\cdot H_2O\}_n$ (2). A mixture of H_3bptc (0.053 g, 0.20 mmol) and 4,4'-bpy (0.156 g, 1.00 mmol) in H_2O (5.0 mL) was added to an aqueous solution (12.0 mL) of $Ni(NO_3)_2\cdot 6H_2O$ (0.114 g, 0.50 mmol) and stirred. The resultant solution was heated in a stainless steel reactor with Teflon liner at 120 °C for 168 h. After a period of approximately 12 h cooling to room temperature, green block crystals of 2 (yield *ca.* 80% based on Ni) were obtained, isolated by filtration and washed with water. IR (KBr, cm^{-1}): 3615m, 3442m, 3118m, 2587w, 2367w, 1709s, 1628s, 1570vs, 1408vs, 1373vs, 1224s, 1073m, 923w, 796s, 680m, 623m, 507w. Elemental analysis calcd for $C_{30}H_{26}N_3O_9Ni$: C, 57.08; H, 4.15; N, 6.66. Found: C, 58.21; H, 4.10; N, 6.85.

Synthesis of $\{[Cd_2(Hbptc)_2(phen)_4]\cdot 3H_2O\}_n$ (3). A mixture of H_3bptc (0.053 g, 0.20 mmol) and phen (0.180 g, 1.00 mmol) in H_2O (5.0 mL) was added to an aqueous solution (12.0 mL) of $Cd(NO_3)_2\cdot 4H_2O$ (0.122 g, 0.50 mmol) and stirred. The resultant solution was heated in a stainless steel reactor with Teflon liner at 120 °C for 120 h. After a period of approximately 12 h cooling to room temperature, colorless block crystals of 3 (yield *ca.* 70% based on Cd) were obtained, isolated by filtration and washed with water. IR (KBr, cm^{-1}): 3049w, 2367w, 1720s, 1547vs, 1407vs, 1373s, 1224s, 1097m, 853s, 726s, 645w, 506w. Elemental analysis calcd for $C_{78}H_{54}N_8O_{15}Cd_2$ (%): C, 59.74; H, 3.47; N, 7.15. Found: C, 62.12; H, 3.25; N, 7.45.

Synthesis of $\{[Cu_2(Hbptc)_2(2,2'-bpy)_2(H_2O)_2]\cdot 2H_2O\}_n$ (4). A mixture of H_3bptc (0.027 g, 0.10 mmol) and 2,2'-bpy (0.078 g, 0.50 mmol) in H_2O (5.0 mL) was added to an aqueous solution (12.0 mL) of $Cu(NO_3)_2\cdot 3H_2O$ (0.089 g, 0.50 mmol) and stirred. The resultant solution was heated in a stainless steel reactor with Teflon liner at 120 °C for 72 h. After a period of approximately 12 h cooling to room temperature, blue needle-like crystals of 4 (yield *ca.* 75% based on Cu) were obtained, isolated by filtration and washed with water. IR (KBr, cm^{-1}): 3049w, 2367w, 1709m, 1604vs, 1582vs, 1397s, 1362vs, 1246m, 1038w, 761m, 715w. Elemental analysis calcd for $C_{25}H_{20}N_2O_8Cu$: C, 55.61; H, 3.73; N, 5.19. Found: C, 55.44; H, 3.68; N, 5.25.

Computational details

All of the structures were optimized using the Becke three-parameter Lee–Yang–Parr (B3-LYP) exchange–correlation functional method¹⁵ with the 6-31G(d,p) basis sets¹⁶ (Fig. S1†). The stable configurations of the structures were confirmed using vibrational frequency analysis, in which no imaginary frequency was found for the configuration at the energy minima. The sum of the electronic and thermal free energies was used to compare their stabilities (Table S1†). All calculations were performed using the Gaussian 09 computational package.¹⁷

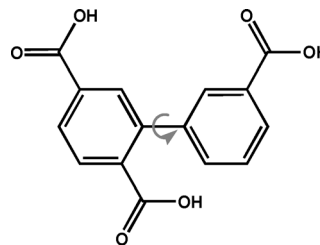
Single-crystal structure determination

The data collection and structural analysis of the crystals, 1–4, were performed using a SMART (Bruker, 2002) diffractometer equipped with Mo-K α radiation ($\lambda = 0.71073 \text{ \AA}$) at 296(2) K. Absorption corrections were applied using multi-scan program SADABS. The structures were solved using direct methods and refined with a full-matrix least-squares technique using the SHELXTL program package.¹⁸ Anisotropic thermal parameters were applied to all non-hydrogen atoms. The organic hydrogen atoms were generated geometrically (C–H 0.96 \AA), the water hydrogen atoms were located using difference maps and refined using isotropic temperature factors. The crystal data as well as details of the data collection and refinements are summarized in Table 1. Selected bond lengths and bond angles are listed in Table S2.† Crystallographic data for the structures reported in this paper have been deposited in the Cambridge Crystallographic Data Center with the CCDC reference numbers 996435–996438 for compounds 1–4.

Results and discussion

Theoretical calculations on free H₃bptc and coordination modes of the deprotonated bptc³⁻/Hbptc²⁻

The biphenyl-3,2',5'-tricarboxylic acid (H₃bptc) has a rotatable coordination vertex and an asymmetric geometry with three carboxylate groups (Scheme 1). The main conformational degrees of the free H₃bptc involve the rotation around the C–C bond between the two phenyl rings. Theoretical calculations show that the thermodynamically most stable conformation in the gas phase is the one with a dihedral angle of 53.5° between the two phenyl rings. The energy of the molecule increases with



Scheme 1 Biphenyl-3,2',5'-tricarboxylic acid (H₃bptc).

changing dihedral angle and reaches a maximum when the phenyl rings are almost co-planar (Fig. S1†).

According to our previous studies on coordination polymers with flexible ligands, the size and the versatile coordination environments of the metal ion may play an important role in controlling the conformation of the flexible ligand.¹¹ In the present H₃bptc system, four metal ions were used, Mn(II), Ni(II), Cd(II) and Cu(II), resulting in different conformations and coordination modes of the ligand (Fig. 1). The dihedral angles between the two phenyl rings in compounds 1–4 are 47.3°, 56.6°, 42.2° and 35.4°, respectively (Table S1†). The fully deprotonated bptc³⁻ ligand in compound 1 adopts a $\mu_5:\eta^2,\eta^2,\eta^1$ bridging mode, while the partly deprotonated Hbptc²⁻ ligands adopt a $\mu_2:\eta^1,\eta^1$ bridging mode in compounds 2 and 4, and a $\mu_2:\eta^2$ bridging mode in compound 3. It should be noted that the different conformations and coordination modes of the ligand not only relate to the metal ions, but also to the auxiliary ligands.

Structure description

$\{[\text{Mn}_3(\text{bptc})_2(4,4'\text{-bpy})_3(\text{H}_2\text{O})_2]\}_n$ (1). The X-ray crystallographic study of 1 revealed an infinite 3D coordination

Table 1 Crystallographic data and refinement parameters for compounds 1–4

Compound	1	2	3	4
Empirical formula	C ₆₀ H ₄₂ N ₆ O ₁₄ Mn ₃	C ₃₀ H ₂₆ N ₃ O ₉ Ni	C ₇₈ H ₅₄ N ₈ O ₁₅ Cd ₂	C ₅₀ H ₄₀ N ₄ O ₁₆ Cu ₂
Fw	1235.82	631.25	1568.09	1079.94
Crystal system	Monoclinic	Triclinic	Monoclinic	Triclinic
Space group	<i>P</i> 2 ₁ / <i>n</i>	<i>P</i> $\bar{1}$	<i>C</i> 2/ <i>c</i>	<i>P</i> $\bar{1}$
<i>a</i> (Å)	9.3553(2)	9.5251(6)	25.6565(6)	7.4683(10)
<i>b</i> (Å)	24.7637(4)	9.8837(6)	12.4636(3)	9.9602(2)
<i>c</i> (Å)	11.6174(2)	16.3942(11)	21.2198(6)	15.8627(3)
α (°)	90.00	72.834(4)	90.00	81.110(10)
β (°)	113.4110(10)	87.431(4)	105.910(2)	88.078(10)
γ (°)	90.00	71.093(4)	90.00	69.099(10)
<i>V</i> (Å ³)	2469.86(8)	1392.88(15)	6525.6(3)	1088.78(3)
<i>Z</i>	2	2	4	1
<i>D</i> _c (g cm ⁻³)	1.662	1.505	1.596	1.647
μ (mm ⁻¹)	0.838	0.759	0.732	1.062
<i>F</i> (000)	1262	654	3176	554
Reflections collected	39 660	22 494	24 648	17 461
<i>R</i> _{int}	0.0465	0.0385	0.0702	0.0286
Gof	1.047	1.062	0.985	1.034
Final <i>R</i> indices	<i>R</i> ₁ ^a = 0.0344	<i>R</i> ₁ ^a = 0.0388	<i>R</i> ₁ ^a = 0.0440	<i>R</i> ₁ ^a = 0.0319
[<i>I</i> > 2 σ (<i>I</i>)]	w <i>R</i> ₂ ^b = 0.0814	w <i>R</i> ₂ ^b = 0.0936	w <i>R</i> ₂ ^b = 0.0867	w <i>R</i> ₂ ^b = 0.0835
<i>R</i> indices (all data)	<i>R</i> ₁ ^a = 0.0513	<i>R</i> ₁ ^a = 0.0566	<i>R</i> ₁ ^a = 0.0785	<i>R</i> ₁ ^a = 0.0395
	w <i>R</i> ₂ ^b = 0.0881	w <i>R</i> ₂ ^b = 0.1062	w <i>R</i> ₂ ^b = 0.0964	w <i>R</i> ₂ ^b = 0.0876
CCDC number	996438	996437	996435	996436

$$^a R_1 = \frac{\sum ||F_o| - |F_c||}{\sum |F_o|}, \quad ^b wR_2 = \frac{[\sum w(F_o^2 - F_c^2)^2 / \sum w(F_o^2)]^{1/2}}{\sum w(F_o^2)}$$

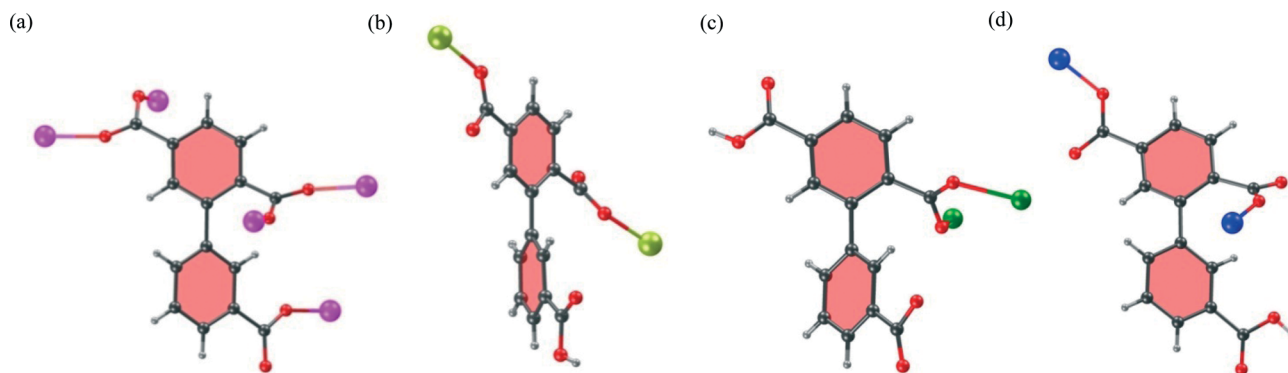


Fig. 1 The coordination modes of $\text{bptc}^{3-}/\text{Hbptc}^{2-}$ in the compounds 1 (a), 2 (b), 3 (c) and 4 (d).

network based on a linear $\text{Mn}(\text{II})_3$ -subunit that crystallizes in the monoclinic space group $P2_1/n$. The asymmetric unit contains two crystallographically different $\text{Mn}(\text{II})$ atoms (one of which lies in an inversion centre), one deprotonated bptc^{3-} ligand, two 4,4'-bpy ligands (one of which lies in an inversion centre), and one coordinated water molecule (Fig. 2a). Mn1 adopts a slightly distorted octahedral geometry, coordinating to three carboxylate oxygen atoms (O1, O4A, O6B) from three bptc^{3-} ligands, to one water oxygen atom (O1W), and two nitrogen atoms (N1, N2C) from two different 4,4'-bpy ligands. Mn2 lies in an inversion centre and also adopts an octahedral geometry, coordinating to four carboxylate oxygen atoms (O2, O5B, O2D, O5E) from four bptc^{3-} and two nitrogen atoms (N3, N3D) from two symmetric 4,4'-bpy ligands. The bond lengths of $\text{Mn}-\text{O}(\text{carboxylate})$ fall in the range of 2.1383(15)–2.2055(13) Å, the axial $\text{Mn}-\text{O}(\text{water})$ bond length is 2.2767(17) Å, and the bond lengths of $\text{Mn}-\text{N}$ are in the range of 2.2691(15)–2.2740(15) Å (Table S2†). The bptc^{3-} ligand with a dihedral angle of 47.3° between the two phenyl rings is fully deprotonated. The three deprotonated carboxylate groups have different coordination modes, including monodentate and bridging $\mu_2-\eta^1:\eta^1$ modes, to link five $\text{Mn}(\text{II})$ atoms (Fig. 1a). The bridging carboxylate groups from four different ligands bind three $\text{Mn}(\text{II})$ atoms, forming a linear $\text{Mn}(\text{II})_3$ -building unit (Fig. 2b). Each trinuclear unit connects six bptc^{3-} ligands (Fig. 2b), while each of the two bptc^{3-} ligands connect four trinuclear units (Fig. 2c). The trinuclear subunits are linked by μ_5 -bridging bptc^{3-} ligands to form a 3D coordination network (Fig. 2d). Meanwhile, there are two kinds of bridging 4,4'-bpy ligands, one of which lies across a 2-fold axis and the other is asymmetric with a dihedral angle of 29.2° between the two pyridyl rings. A 3D condensed framework is thus generated by the connection of the bptc^{3-} and 4,4'-bpy ligands with no lattice water molecules (Fig. 2e). There are intramolecular hydrogen bonds between the coordinated water and the uncoordinated carboxylate groups ($\text{O1W}\cdots\text{O3}$ $a = 2.698(2)$ Å, $\text{O1W}-\text{H1WA}\cdots\text{O3}$ $a = 170(4)^\circ$, $a: x, y, z + 1$).

$\{[\text{Ni}(\text{Hbptc})(4,4'\text{-bpy})_{1.5}(\text{H}_2\text{O})_2]\cdot\text{H}_2\text{O}\}_n$ (2). The X-ray crystallographic study of 2 revealed a supramolecular network, based on 1D coordinated ladder chains, that crystallizes in the triclinic space group $P\bar{1}$. The asymmetric unit contains one

crystallographic type of $\text{Ni}(\text{II})$ atom, one partly deprotonated Hbptc^{2-} ligand, two 4,4'-bpy ligands (one of which lies in an inversion centre), two coordinated and one lattice water molecule (Fig. 3a). Ni1 adopts a slightly distorted octahedral geometry, coordinating to two carboxylate oxygen atoms (O2, O3A) from two Hbptc^{2-} ligands, to two water oxygen atoms (O1W, O2W), and two nitrogen atoms (N1, N3) from two different 4,4'-bpy ligands. The $\text{Ni}-\text{N}$ bond lengths are 2.0596(18) and 2.0943(19) Å, $\text{Ni}-\text{O}(\text{water})$ 2.0908(17) and 2.0921(18) Å, and $\text{Ni}-\text{O}(\text{carboxylate})$ 2.0597(15) and 2.0634(15) Å (Table S2†). The Hbptc^{2-} ligand with a dihedral angle of 56.6° between the two phenyl rings is partly deprotonated at the 2',5'-carboxylate groups (Fig. 1b). The partly deprotonated Hbptc^{2-} adopts a μ_2 -bridging coordination mode through two deprotonated carboxylate groups on the same phenyl ring, connecting the $\text{Ni}(\text{II})$ atoms to form a 1D $\text{Ni}-\text{Hbptc}$ chain (Fig. 3b). There are two kinds of 4,4'-bpy ligands adopting a monodentate and a μ_2 -bridging coordination mode, respectively. The μ_2 -bridging 4,4'-bpy ligand, lying in an inversion centre, connects two $\text{Ni}-\text{Hbptc}$ chains to form a 1D ladder chain, and the monodentate 4,4'-bpy ligands, with a dihedral angle of 20.6° between the two pyridyl rings, are arrayed along both sides of the chain (Fig. 3b). The ladder chains are zipped together through their uncoordinated carboxylate groups and the monodentate 4,4'-bpy *via* hydrogen bonds (Fig. 3c). Thus, a 3D supramolecular network, with 1D channels occupied by water molecules, is generated (Fig. 3d) and further strengthened by rich hydrogen bonds between the carboxylate groups, 4,4'-bpy and the water molecules. ($\text{O}\cdots\text{O} = 2.664(3)\text{--}3.137(3)$ Å, $\text{O}-\text{H}\cdots\text{O} = 151\text{--}172^\circ$) (Table S3†).

$\{[\text{Cd}_2(\text{Hbptc})_2(\text{phen})_4]\cdot 3\text{H}_2\text{O}\}_n$ (3). The X-ray crystallographic study revealed that 3 crystallizes in the monoclinic $C2/c$ space group. The asymmetric unit contains one crystallographic type of $\text{Cd}(\text{II})$ atom, one partly deprotonated Hbptc^{2-} ligand, two phen ligands and three disordered lattice water molecules. Cd1 lies on a general position and has a six-coordinated distorted octahedral geometry, coordinating to two carboxylate oxygen atoms (O1, O2A) from two Hbptc^{2-} ligands and to four nitrogen atoms (N1, N2, N3, N4) from two phen ligands (Fig. 4a). The bond lengths of $\text{Cd}-\text{O}$ are 2.246(2) and 2.270(3) Å and those of $\text{Cd}-\text{N}$ fall between 2.298(3) and

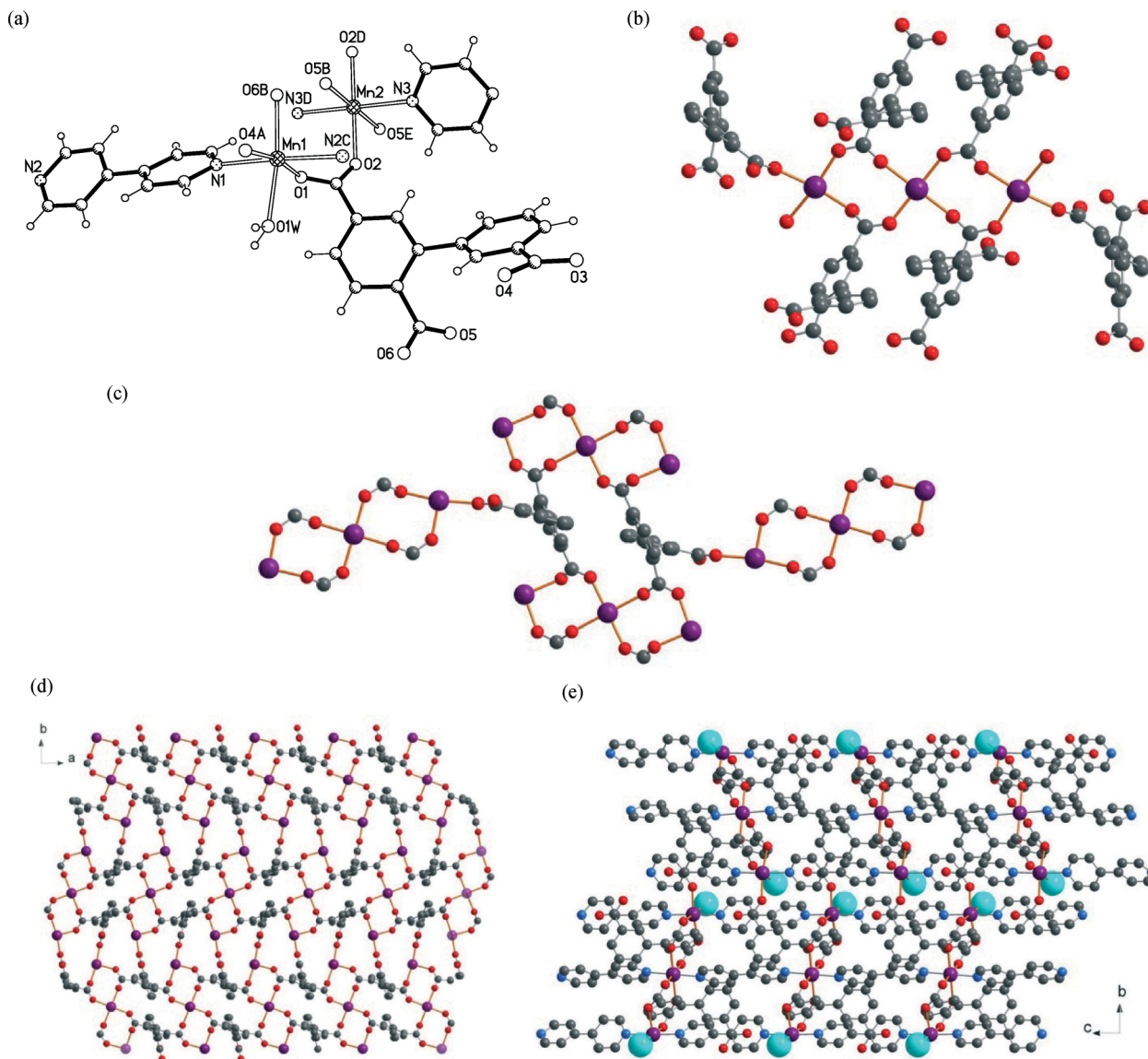


Fig. 2 (a) View of the coordination environments around the Mn(II) atoms in **1** (A: $x - 1/2, -y + 1/2, z + 1/2$; B: $x - 1, y, z$; C: $x, y, z - 1$; D: $-x, -y, -z$; E: $-x + 1, -y, -z$); (b) the linear Mn(II)₃-building unit; (c) the coordination of each of the two bptc³⁻ ligands surrounded by four linear Mn(II)₃-subunits; (d) the 3D coordination network with bridging bptc³⁻ ligands along the *c*-axis (4,4'-bpy ligands are omitted for clarity); (e) the 3D coordination framework with bridging bptc³⁻ and 4,4'-bpy ligands (the coordinated water molecules in the framework are highlighted as sky blue spheres).

2.432(3) Å (Table S2†). The Hbptc²⁻ ligand, with a dihedral angle of 42.2° between the two phenyl rings, is partly deprotonated at the 3,2'-carboxylate groups (Fig. 1c). The partly deprotonated Hbptc²⁻ connects two Cd(II) atoms in a μ_2 -bridging coordination mode through its deprotonated 2'-carboxylate group. Two Hbptc²⁻ ligands and four phen ligands connect two Cd(II) atoms to form a dimer building block [Cd₂(Hbptc)₂(phen)₄], which lies in an inversion centre (Fig. 4b). The dimers are connected with each other to form a 1D chain *via* hydrogen bonds between the deprotonated and protonated carboxylate groups. Furthermore, the adjacent chains are held together *via* $\pi \cdots \pi$ interactions between the phen ligands, forming a 3D supramolecular network (Fig. 4c). The shortest distance between the two parallel phen planes is

3.7 Å, which is within the common range of $\pi \cdots \pi$ interactions between the two phenyl rings. There are hydrogen bonds between the partly deprotonated carboxylate groups with shared hydrogen atoms (O4 \cdots O4 $a = 2.430(5)$ Å, O4-H \cdots O4 $a = 115^\circ$, $a: -x, y, -z + 3/2$). The three disordered lattice water molecules are removed using the SQUEEZE procedure and can be easily lost above room temperature because of the hydrophobic effect of the molecules.

$\{[\text{Cu}_2(\text{Hbptc})_2(2,2'\text{-bpy})_2(\text{H}_2\text{O})_2] \cdot 2\text{H}_2\text{O}\}_n$ (**4**). The X-ray crystallographic study of **4** revealed a supramolecular network, based on [Cu₂(Hbptc)₂(2,2'-bpy)₂] dimers, that crystallizes in the triclinic space group $P\bar{1}$. The asymmetric unit contains one crystallographic type of Cu(II) atom, one partly deprotonated Hbptc²⁻ ligand, one 2,2'-bpy ligand, one coordinated and one

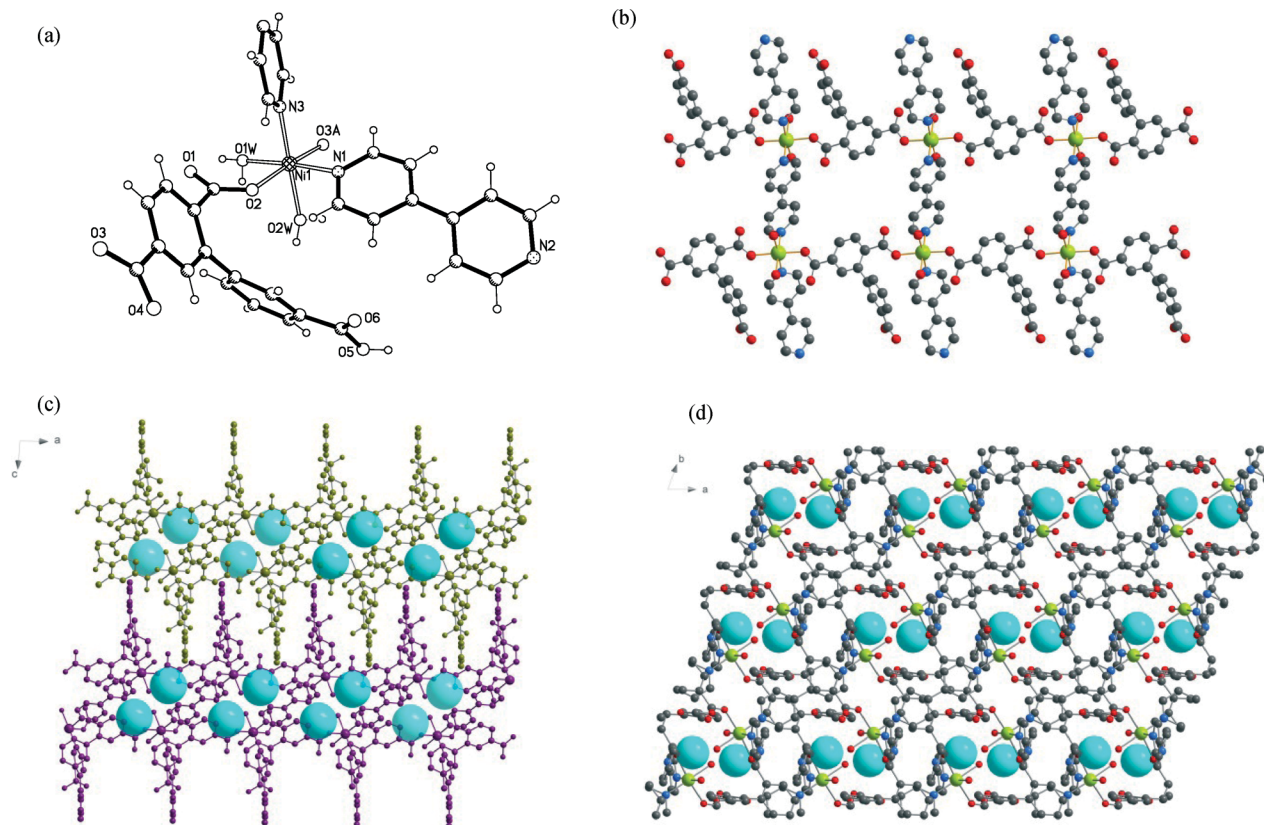


Fig. 3 (a) View of the coordination environment around the Ni(II) atom in **2** (A: $x + 1, y - 1, z$); (b) the 1D ladder chain with bridging Hbptc²⁻ and 4,4'-bpy ligands; (c) the adjacent ladder chains zipped together through their uncoordinated carboxylate groups and monodentate 4,4'-bpy by hydrogen bonds viewed along the *b*-axis (the lattice water molecules are highlighted in sky blue spheres); (d) the 3D supramolecular framework with 1D channels, viewed along the *c*-axis (the lattice water molecules in the channels are highlighted by sky blue spheres).

lattice water molecule. Cu1 adopts a slightly distorted tetragonal pyramidal geometry, coordinating to two carboxylate oxygen atoms (O2, O4A) from two Hbptc²⁻ ligands, to one water oxygen atom (O1W), and to two nitrogen atoms (N1, N2) from one 2,2'-bpy ligand (Fig. 5a). The bond lengths of Cu–N are 1.9929(16) and 2.0089(16) Å. The axial Cu–O(water) bond length (2.2187(15) Å) is much longer than the equatorial Cu–O(carboxylate) ones (1.9115(13) and 1.9904(13) Å) (Table S2†). The Hbptc²⁻ ligand, with a dihedral angle of 35.4° between the two phenyl rings, is partly deprotonated at the 2',5'-carboxylate groups (Fig. 1d). The partly deprotonated Hbptc²⁻ ligand connects two Cu(II) atoms in a μ_2 -bridging coordination mode through two deprotonated carboxylate groups. Two Hbptc²⁻ ligands and two 2,2'-bpy ligands connect two Cu(II) atoms to form a dimer building block, which lies in an inversion centre (Fig. 5b). Due to the different bridging modes of the Hbptc²⁻ ligand in **3** and **4**, the Cu \cdots Cu distance of 9.4 Å in the [Cu₂(Hbptc)₂(2,2'-bpy)₂] dimer is much longer than the Cd \cdots Cd distance of 4.6 Å in the [Cd₂(Hbptc)₂(phen)₄] dimer. The adjacent dimers are held together *via* $\pi\cdots\pi$ interactions to form a 1D chain with a distance of 3.3 Å between the phenyl ring of the Hbptc²⁻ ligand and the pyridyl ring of 2,2'-bpy (Fig. 5c). Furthermore, rich hydrogen bonds between the water molecules and the carboxylate groups connect the chains, forming

a 3D supramolecular network (O \cdots O = 2.638(3)–3.023(2) Å, O–H \cdots O = 157(4)–175(2)°) (Table S3†).

Thermal stability analysis

The XRPD measurements were carried out at room temperature to confirm the phase purity of compounds **1–4**. As shown in Fig. S2,† the peak positions of the simulated and experimental XRPD patterns are in agreement with each other, demonstrating the good phase purity of the four compounds.

In order to examine the thermal stabilities of the four compounds, the thermal gravimetric (TG) analyses were carried out under a dry nitrogen atmosphere from 30 to 650 °C (Fig. S3†). For compound **1**, the TGA curve shows that the first weight loss of 3.0% at the beginning from 80 °C to 140 °C corresponds to the loss of the coordinated water molecule (calcd 2.9%) of one unit cell. The network is decomposed at 300 °C. The remaining weight of 17.2% indicates that the final product is MnO (calcd 17.2%). Compound **2** loses the lattice and coordinated water molecules (calcd 8.7% and expt 8.8%) from the beginning to 150 °C, and then the supramolecular network is decomposed quickly, resulting in residual NiO (calcd 11.8% and expt 10.0%). For compound **3**, two disordered water molecules have been lost at room temperature

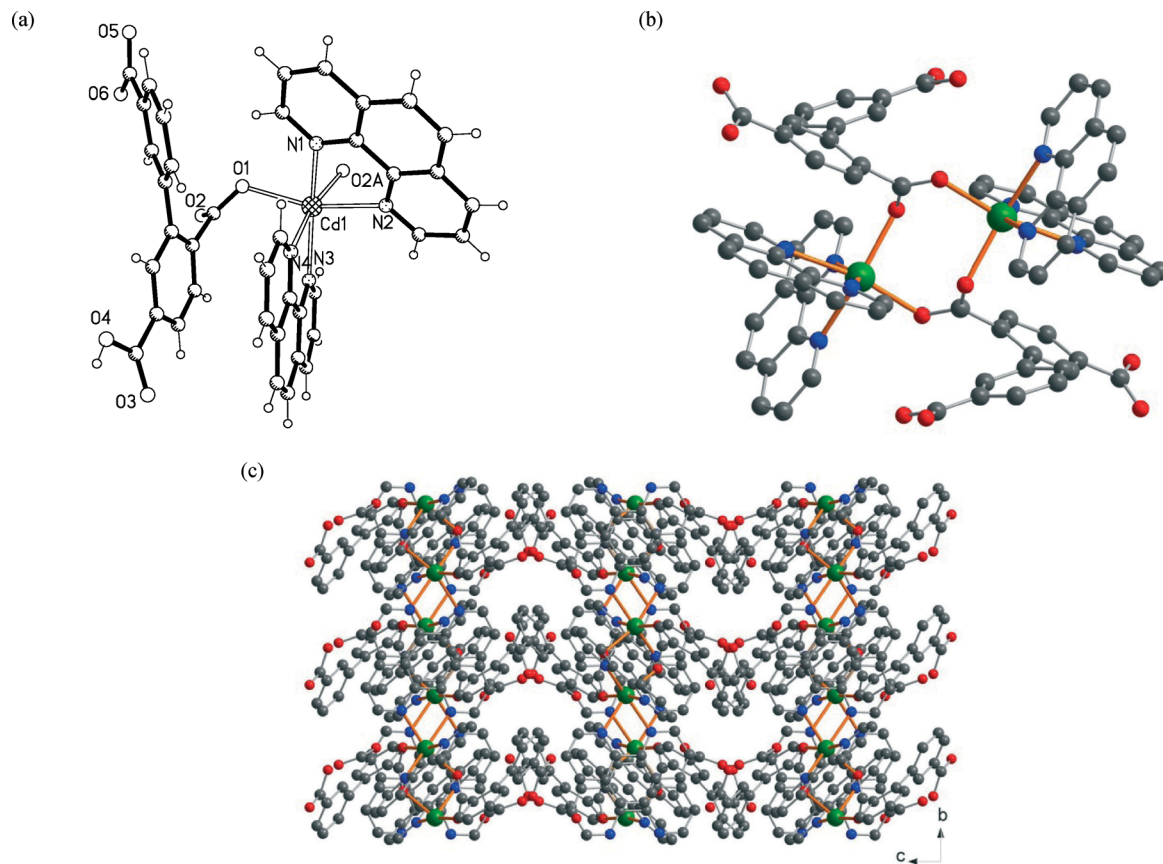


Fig. 4 (a) View of the coordination environment around the Cd(II) atom in **3** ($A: -x + 1/2, -y + 3/2, -z + 1$); (b) the dimer building block $[\text{Cd}_2(\text{Hbptc})_2(\text{phen})_4]$; (c) the 3D packed supramolecular network, held together via $\pi \cdots \pi$ interactions, viewed along the a -axis.

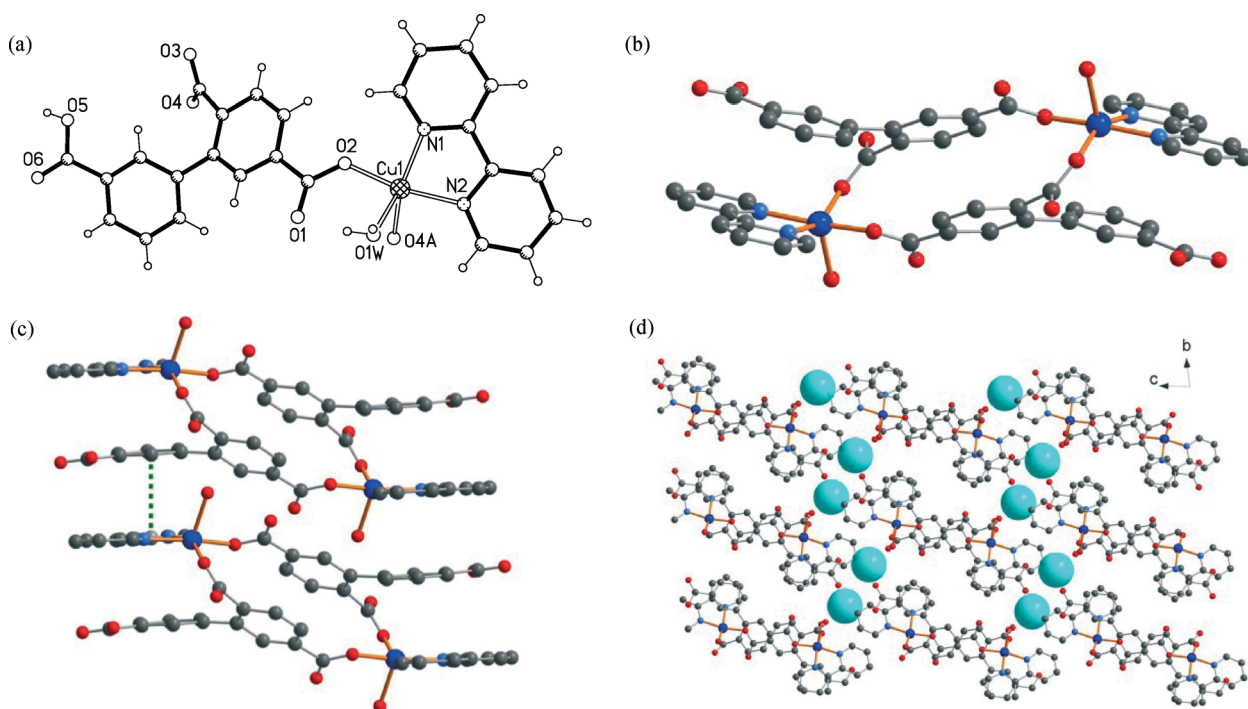


Fig. 5 (a) View of the coordination environment around the Cu(II) atom in **4** ($A: -x + 2, -y + 1, -z + 1$); (b) the dimer building block $[\text{Cu}_2(\text{Hbptc})_2(2,2'\text{-bpy})_2]$; (c) the $\pi \cdots \pi$ interactions between the phenyl and the pyridyl rings from adjacent dimers (the hydrogen atoms are omitted for clarity); (d) the stacked supramolecular network with lattice water molecules, viewed along the a -axis (the lattice water molecules in the channels are highlighted by sky blue spheres).

because of the hydrophobic effect of the molecules. The third water molecule (calcd 1.1% and expt 1.1%) was lost from the beginning to 80 °C and the network collapsed in the temperature range 280–620 °C, which indicates that it is thermally stable over a wide temperature range. The observed weight losses include three steps between 280 °C and 620 °C before the final formation of CdO, which can be assigned to the elimination of the phen and Hbpt²⁻ ligands. For compound 4, the TGA curve shows that the first weight loss of 3.2% from the beginning to 90 °C corresponds to the loss of the lattice water molecule (calcd 3.3%) of one unit cell, the coordinated water molecule is lost at temperatures up to 150 °C. The network is stable between 150 °C to 265 °C and then collapses quickly before the final formation of the metal oxide.

Magnetic properties

The variable temperature magnetic susceptibility was measured for compound 1 in a 1 kOe dc field. At 300 K, the experimental $\chi_M T$ value is 13.0 cm³ mol⁻¹ K, which is consistent with the expected value (13.125 cm³ mol⁻¹ K) for three Mn(II) ions ($S = 5/2$, $g = 2$) (Fig. 6a). Upon cooling, the $\chi_M T$ value steadily decreases to 3.89 cm³ mol⁻¹ K at 1.8 K. Fitting the experimental data to the Curie–Weiss law in the temperature range of 10–300 K leads to an antiferromagnetic Weiss constant of $\theta = -7.1$ K (Fig. 6b). The dominating antiferromagnetic interactions in 1 are also implied by the unsaturated magnetization values of 11.6 N β at 2 K and 70 kOe (compared with the expected 15 N β) (Fig. 6c). Moreover, due to the symmetrical linear Mn(II) trimer sub-structure of 1, the magnetic susceptibility can also be satisfactorily fitted to the exchange model using the spin Hamiltonian:¹⁹

$$\hat{H} = -2 \sum_{i=1}^n \sum_{j>i}^n J_{ij} \vec{S}_i \cdot \vec{S}_j$$

The results reveal an intra-trimer $J = -0.475(4)$ cm⁻¹ and an inter-trimer $zJ = -0.027(2)$ cm⁻¹ with $g = 2.007(1)$, indicating weak antiferromagnetic interactions both inside (Mn···Mn = 5.0 Å) and among (Mn···Mn = 9.4 Å) the Mn(II)₃ sub-structures, compared to the reported linear Mn(II)₃-based coordination polymers.²⁰

On the other hand, the magnetic properties of 2 and 4 mainly come from the single-ion behavior of Ni(II) and Cu(II), respectively, owing to the lack of strong magnetic interactions as in 1. At 300 K, the $\chi_M T$ values are 1.31 cm³ mol⁻¹ K for 2 (Fig. 7a) and 0.43 cm³ mol⁻¹ K for 4 (Fig. 7b). Both of them are larger than the spin-only values (1.0 for 2 and 0.375 for 4), indicating the presence of spin–orbit coupling which is commonly observed for Ni(II) and Cu(II).^{19,21} Upon cooling, the $\chi_M T$ values decrease slowly, mainly owing to the weak antiferromagnetic interactions and/or zero-field splitting. Fitting the experimental data to the Curie–Weiss law in the range of 1.8–300 K leads to the negative Weiss constants of $\theta = -0.83$ K for 2 and -0.54 K for 4, both of which are much smaller in their absolute value than that of 1. The magnetization curves at 2 K also show a typical paramagnetic

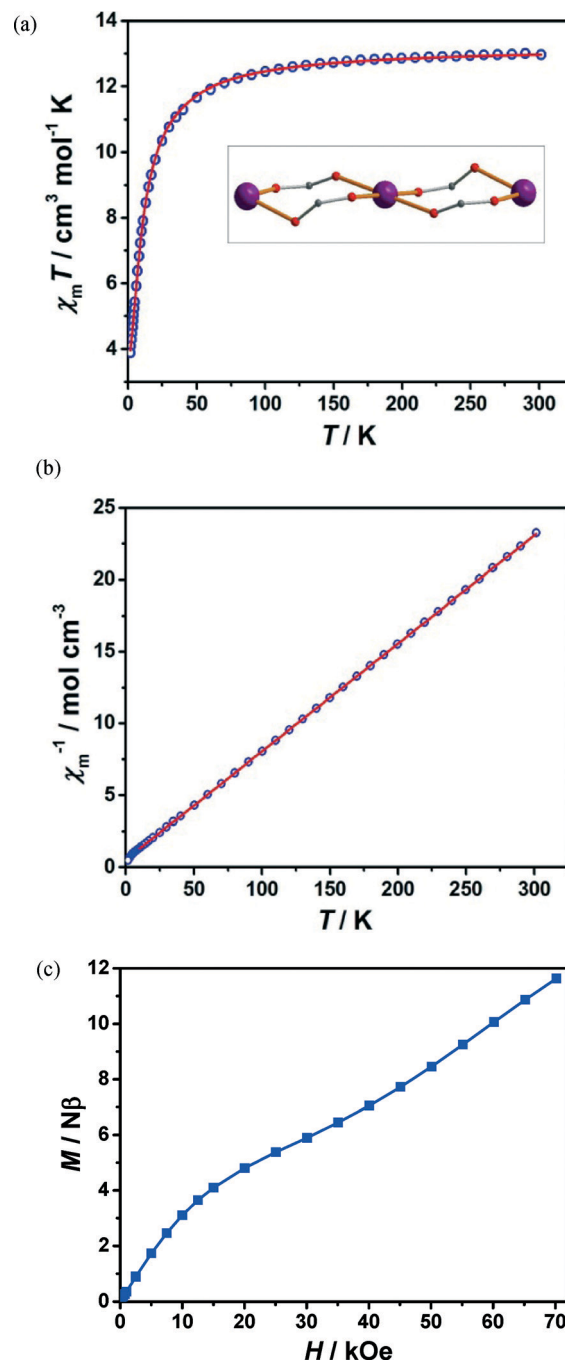


Fig. 6 (a) The temperature-dependence of $\chi_M T$ in the range of 1.8–300 K (the solid line is fitted to the exchange model, the insert is the scheme of the Mn(II)₃-subunit); (b) the temperature-dependence of χ_M^{-1} (the solid line is fitted to the Curie–Weiss law); and (c) the field-dependent magnetization at 2 K (the solid line is a guide to the eye), for 1.

shape as expected, reaching a saturation of 2.29 N β for 2 and 1.00 N β for 4 (Fig. 7c).

Luminescent properties

The solid-state luminescent properties of the free H₃bptc ligand and compound 3 were investigated in the solid state at room temperature. The emission band, with a maximum

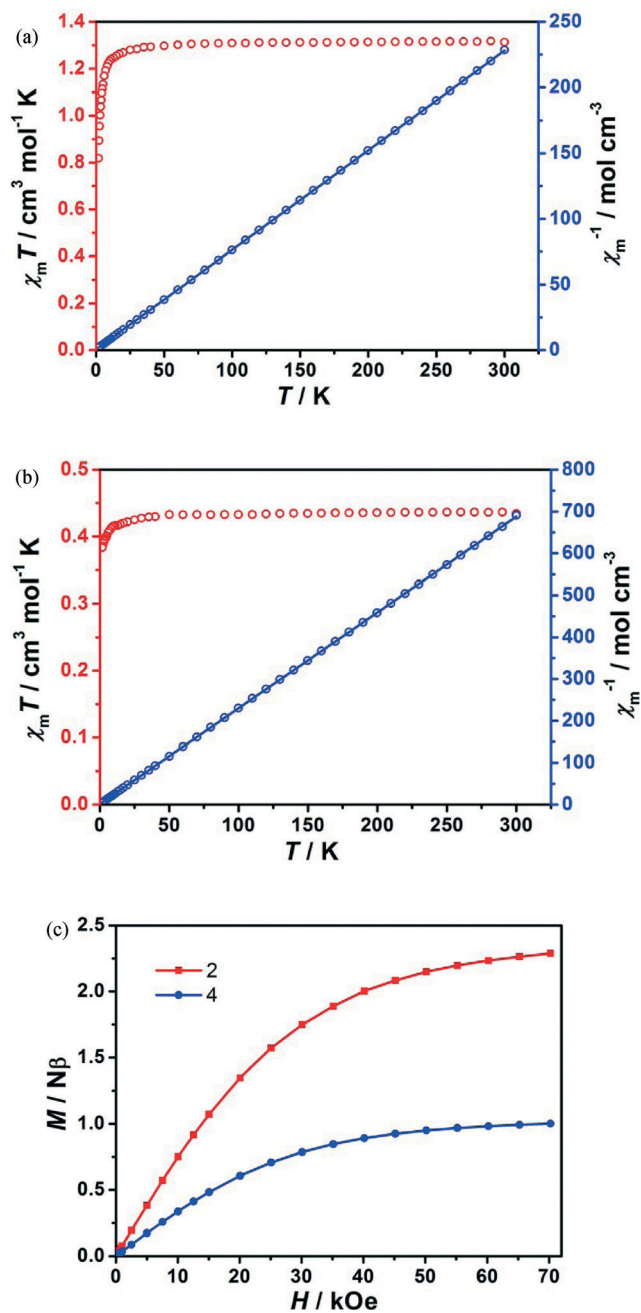


Fig. 7 (a) The temperature-dependence of $\chi_M T$ (left) and χ_M^{-1} (right) in the range of 1.8–300 K (the solid line is fitted to the Curie–Weiss law) for 2; (b) the temperature-dependence of $\chi_M T$ (left) and χ_M^{-1} (right) in the range of 2–300 K (the solid line is fitted to the Curie–Weiss law) for 4; and (c) the field-dependent magnetization at 2 K for 2 (red) and 4 (blue) (the solid lines are a guide to the eye).

observed at 484 nm upon excitation at 296 nm, for H_3bptc can be attributed to the $\pi^* \rightarrow n$ or $\pi^* \rightarrow \pi$ transition (Fig. 8a).^{1c,22} According to the reported literature, the free phen molecule displays strong emission around 390 nm in the solid state at room temperature, attributed to the $\pi^* \rightarrow \pi$ transition.^{7a,23} Comparably, the emission of compound 3, observed at 453 nm ($\lambda_{\text{ex}} = 365$ nm) with a blue-shift of 31 nm (compared to free H_3bptc) and a red shift of *ca.* 40 nm

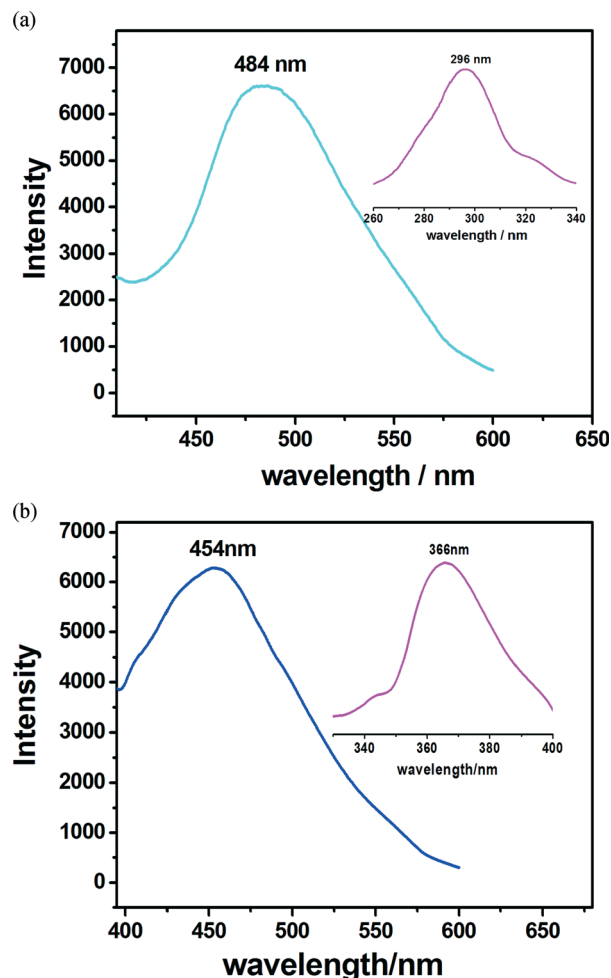


Fig. 8 The excitation (insert) and emission spectra of (a) the free H_3bptc ligand and (b) compound 3 in the solid state at room temperature.

(compared to free phen), can be assigned to the cooperative effect of the metal-perturbed intra-ligand emission between H_3bptc and phen (Fig. 8b).²⁴ Notably, the chelation of the H_3bptc ligand to metal ions can effectively change the dihedral angle between the two phenyl rings, and reduce the loss of energy produced by the radiationless decay.²⁴ Thus, the enhancement and blue-shift in compound 3 may be attributed to the altered energy level of the $\pi^* \rightarrow n$ or $\pi^* \rightarrow \pi$ transition. Different from compound 3 with a d^{10} configuration, the emission bands of compound 1, 2, and 4 with unpaired electrons are observed around 498 nm and 520 nm with weak intensities (Fig. S4†), which may be due to the ligand-field transitions ($d-d$) *via* electrons, or the energy transfer *via* the partially filled d-orbitals.²⁵

Conclusions

Four new coordination polymers, involving an asymmetric ligand with a rotatable coordination vertex and N-donor

ligands, have been successfully synthesized and characterized. According to single crystal X-ray analysis, compound 1 forms a 3D coordination network, 2 forms a 1D ladder chain-based structure, and 3 and 4 form 0D dimer-based structures. The asymmetric H₃bptc ligand has been partly or fully deprotonated and adopts different coordination modes in these compounds. Theoretical calculations on the free H₃bptc ligand show that the thermodynamically most stable conformation is the one with a dihedral angle of 53.5°, while the dihedral angles are 47.3°, 56.6°, 42.2° and 35.4° in compounds 1–4, respectively. The observed weight losses include three steps between 280 °C and 620 °C before the final formation of CdO, which can be assigned to the elimination of the phen and Hbpt²⁻ ligands. Magnetic property studies indicated the existence of antiferromagnetic interactions in compounds 1, 2 and 4. Luminescent property studies revealed that compound 3 displays an intense blue emission in the solid state at room temperature, which may be a good candidate for potential photoactive materials.

Acknowledgements

This work was supported by the National Science Foundation of China (no. 20901018) and the Yang-cheng Scholars Foundation of Guangzhou (no. 12A002D).

Notes and references

- (a) H.-X. Deng, C. J. Doonan, H. Furukawa, R. B. Ferreira, J. Towne, C. B. Knobler, B. Wang and O. M. Yaghi, *Science*, 2010, **327**, 846; (b) L. E. Kreno, K. Leong, O. K. Farha, M. Allendorf, R. P. V. Duyne and J. T. Hupp, *Chem. Rev.*, 2012, **112**, 1105; (c) Y.-J. Cui, Y.-F. Yue, G.-D. Qian and B.-L. Chen, *Chem. Rev.*, 2012, **112**, 1126; (d) T. Yamada, K. Otsubo, R. Makiura and H. Kitagawa, *Chem. Soc. Rev.*, 2013, **42**, 6655; (e) M. Zhao, S. Ou and C.-D. Wu, *Acc. Chem. Res.*, 2014, **47**, 1199; (f) S.-H. Yang, X. Lin, W. Lewis, M. Suyetin, E. Bichoutskaia, J. E. Parker, C. C. Tang, D. R. Allan, P. J. Rizkallah, P. Hubberstey, N. R. Champness, K. M. Thomas, A. J. Blake and M. Schröder, *Nat. Mater.*, 2012, **11**, 710; (g) M. H. Mohamed, S. Elsaidi, L. Wojtas, T. Pham, K. A. Forrest, B. Tudor, B. Space and M. J. Zawarotko, *J. Am. Chem. Soc.*, 2012, **134**, 19556; (h) X. Bao, H. J. Shepherd, L. Salmon, G. Molnar, M.-L. Tong and A. Bousseksou, *Angew. Chem., Int. Ed.*, 2013, **52**, 1198.
- (a) D. Yuan, D. Zhao, D. Sun and H.-C. Zhou, *Angew. Chem., Int. Ed.*, 2010, **49**, 5357; (b) Q.-K. Liu, J.-P. Ma and Y.-B. Dong, *J. Am. Chem. Soc.*, 2010, **132**, 7005; (c) Y. Yan, S. Yang, A. J. Blake, W. Lewis, E. Poirier, S. A. Barnett, N. R. Champness and M. Schröder, *Chem. Commun.*, 2011, **47**, 9995; (d) D. Sun, Z.-H. Yan, V. A. Blatov, L. Wang and D.-F. Sun, *Cryst. Growth Des.*, 2013, **13**, 1277; (e) L.-H. Cao, Y.-L. Wei, Y. Yang, H. Xu, S.-Q. Zang, H.-W. Hou and T. C. W. Mak, *Cryst. Growth Des.*, 2014, **14**, 1827; (f) L. Ma, N. Yu, S. Chen and H. Deng, *CrystEngComm*, 2013, **15**, 1352; (g) F. Guo, B. Zhu, M. Liu, X. Zhang, J. Zhang and J. Zhao, *CrystEngComm*, 2013, **15**, 6191; (h) Z. Wu, W. Sun, Y. Chai, W. Zhao, H. Wu, T. Shi and X. Yang, *CrystEngComm*, 2014, **16**, 406; (i) Z.-J. Lin and M.-L. Tong, *Coord. Chem. Rev.*, 2011, **255**, 421.
- (a) D. Tian, Q. Chen, Y. Li, Y.-H. Zhang, Z. Chang and X.-H. Bu, *Angew. Chem.*, 2014, **126**, 856; (b) P. V. Dau, K. K. Tanabe and S. M. Cohen, *Chem. Commun.*, 2013, **49**, 9370; (c) P. V. Dau, M. Kim and S. M. Cohen, *Chem. Sci.*, 2012, **4**, 601; (d) T. Li, J. Yang, X.-J. Hong, Y.-J. Ou, Z.-G. Gu and Y.-P. Cai, *CrystEngComm*, 2014, **16**, 3848; (e) Z.-J. Lin, Y.-B. Huang, T.-F. Liu, X.-Y. Li and R. Cao, *Inorg. Chem.*, 2013, **52**, 3127; (f) S.-Q. Su, S. Wang, X.-Z. Song, S.-Y. Song, C. Qin, M. Zhu, Z.-M. Hao, S.-N. Zhao and H.-J. Zhang, *Dalton Trans.*, 2012, **41**, 4772.
- (a) Q.-Y. Liu, Y.-L. Li, Y.-L. Wang, C.-M. Liu, L.-W. Ding and Y. Liu, *CrystEngComm*, 2014, **16**, 486; (b) S. Henke, A. Schneemann, S. Kapoor, R. Winter and R. A. Fischer, *J. Mater. Chem.*, 2012, **22**, 909; (c) D. O. Miles, D.-M. Jiang, A. D. Burrows, J. E. Halls and F. Marken, *Electrochem. Commun.*, 2013, **27**, 9; (d) J.-A. Hua, Y. Zhao, Q. Liu, D. Zhao, K. Chen and W.-Y. Sun, *CrystEngComm*, 2014, **16**, 7536.
- (a) L. J. Murray, M. Dinca, J. Yano, S. Chavan, S. Bordiga, C. M. Brown and J. R. Long, *J. Am. Chem. Soc.*, 2010, **132**, 7856; (b) L. Luo, G.-C. Lv, P. Wang, Q. Liu, K. Chen and W.-Y. Sun, *CrystEngComm*, 2013, **15**, 9537; (c) Y.-H. Luo, F.-X. Yue, X.-Y. Yu, L.-L. Gu, H. Zhang and X. Chen, *CrystEngComm*, 2013, **15**, 8116; (d) X. Zhang, Y.-Y. Huang, Q.-P. Lin, J. Zhang and Y.-G. Yao, *Dalton Trans.*, 2013, **42**, 2294; (e) Y.-W. Li, J.-R. Li, L.-F. Wang, B.-Y. Zhou, Q. Chen and X.-H. Bu, *J. Mater. Chem. A*, 2013, **1**, 495.
- (a) W.-J. Ji, Q.-G. Zhai, S.-N. Li, Y.-C. Jiang and M.-C. Hu, *Chem. Commun.*, 2011, **47**, 3834; (b) P. Song, B. Liu, Y.-Q. Li, J.-Z. Yang, Z.-M. Wang and X.-G. Li, *CrystEngComm*, 2012, **14**, 2296; (c) G.-H. Cui, C.-H. He, C.-H. Jiao, J.-C. Geng and V. A. Blatov, *CrystEngComm*, 2012, **14**, 4210; (d) J.-F. Liu, F.-P. Huang, H.-D. Bian and Q. Yu, *Z. Anorg. Allg. Chem.*, 2013, **639**, 2347; (e) E. Yang, Q.-R. Ding, Y. Kang and F. Wang, *Inorg. Chem. Commun.*, 2013, **36**, 195.
- (a) J. Wang, Z.-J. Lin, Y.-C. Ou, N.-L. Yang, Y.-H. Zhang and M.-L. Tong, *Inorg. Chem.*, 2008, **47**, 190; (b) X.-Y. Wang and S. C. Sevov, *Inorg. Chem.*, 2008, **47**, 1037; (c) J. Wang, S.-H. Yang, A.-J. Zhou, Z.-Q. Liu and J. Zhao, *J. Coord. Chem.*, 2013, **66**, 2413.
- (a) S. S.-Y. Chui, A. Siu, X. Feng, Z.-Y. Zhang, T. C. W. Mak and I. D. Williams, *Inorg. Chem. Commun.*, 2001, **4**, 467; (b) H. Kumagai, Y. Oka, M. A. Tanaka and K. Inoue, *Inorg. Chim. Acta*, 2002, **332**, 176; (c) A. Kyono, M. Kimata and T. Hatta, *Inorg. Chim. Acta*, 2004, **357**, 2519; (d) E. Yang, J. Zhang, Z.-J. Li, S. Gao, Y. Kang, Y.-B. Chen, Y.-H. Wen and Y.-G. Yao, *Inorg. Chem.*, 2004, **43**, 6525; (e) S. M. Humphrey, R. A. Mole, R. I. Thompson and P. T. Wood, *Inorg. Chem.*, 2010, **49**, 3441.
- (a) R.-Q. Zhong, R.-Q. Zou, M. Du, T. Yamada, G. Maruta, S. Takeda, J. Li and Q. Xu, *CrystEngComm*, 2010, **12**, 677; (b) S. A. Sapchenko, D. N. Dybtsev, D. G. Samsonenko and V. P. Fedin, *New J. Chem.*, 2010, **34**, 2445; (c) X.-Y. Yi,

- Y. Ying, H.-C. Fang, Z.-G. Gu, S.-R. Zheng, Q.-G. Zhan, L.-S. Jiang, W.-S. Li, F.-Q. Sun and Y.-P. Cai, *Inorg. Chem. Commun.*, 2011, **14**, 453; (d) G.-P. Zhou, Y.-L. Yang, R.-Q. Fan, W.-W. Cao and B. Yang, *CrystEngComm*, 2012, **14**, 193; (e) P. K. Yadav, N. Kumari, P. Pachfule, R. Banerjee and L. Mishra, *Cryst. Growth Des.*, 2012, **12**, 5311; (f) F. Guo, F. Wang, H. Yang, X.-L. Zhang and J. Zhang, *Inorg. Chem.*, 2012, **51**, 9677.
- 10 (a) Z.-J. Lin, B. Xu, T.-F. Liu, M.-N. Cao, J. Lü and R. Cao, *Eur. J. Inorg. Chem.*, 2010, 3842; (b) Z.-Y. Guo, H. Xu, S.-Q. Su, J.-F. Cai, S. Dang, S.-C. Xiang, G.-D. Qian, H.-J. Zhang, M. O. Keeffed and B.-L. Chen, *Chem. Commun.*, 2011, **47**, 5551; (c) Z.-J. Zhang, L.-P. Zhang, L. Wojtas, P. Nugent, M. Eddaoudi and M. J. Zaworotko, *J. Am. Chem. Soc.*, 2012, **134**, 924; (d) L.-N. Li, J.-H. Luo, S.-Y. Wang, Z.-H. Sun, T.-L. Chen and M.-C. Hong, *Cryst. Growth Des.*, 2011, **11**, 3744; (e) C.-C. Ji, J. Li, Y.-Z. Li, Z.-J. Guo and H.-G. Zheng, *CrystEngComm*, 2011, **13**, 459; (f) L.-N. Li, S.-Y. Wang, T.-L. Chen, Z.-H. Sun, J.-H. Luo and M.-C. Hong, *Cryst. Growth Des.*, 2012, **12**, 4109.
- 11 (a) J. Jia, M. Shao, T.-T. Jia, S.-R. Zhu, Y.-M. Zhao, F.-F. Xing and M.-X. Li, *CrystEngComm*, 2010, **12**, 1548; (b) L.-X. Sun, Y. Qi, Y.-M. Wang, Y.-X. Che and J.-M. Zheng, *CrystEngComm*, 2010, **12**, 1540; (c) J. Zhao, D.-S. Li, Z.-Z. Hu, W.-W. Dong, K. Zou and J. Y. Lu, *Inorg. Chem. Commun.*, 2011, **14**, 771; (d) Q.-P. Lin, T. Wu, S.-T. Zheng, X.-H. Bu and P.-Y. Feng, *Chem. Commun.*, 2011, **47**, 11852; (e) I. A. Ibarra, S.-H. Yang, X. Lin, A. J. Blake, P. J. Rizkallah, H. Nowell, D. R. Allan, N. R. Champness, P. Hubberstey and M. Schröder, *Chem. Commun.*, 2011, **47**, 8304; (f) X.-T. Zhang, L.-M. Fan, Z. Sun, W. Zhang, D.-C. Li, J.-M. Dou and L. Han, *Cryst. Growth Des.*, 2013, **13**, 792; (g) J. Zhao, D.-S. Li, X.-J. Ke, B. Liu, K. Zou and H.-M. Hu, *Dalton Trans.*, 2012, **41**, 2560; (h) S.-H. Yang, J.-L. Sun, A. J. Ramirez-Cuesta, S. K. Callear, W. I. F. David, D. P. Anderson, R. Newby, A. J. Blake, J. E. Parker, C. C. Tang and M. Schröder, *Nat. Chem.*, 2012, **4**, 887; (i) S.-H. Yang, A. J. Ramirez-Cuesta and M. Schröder, *Chem. Phys.*, 2014, **428**, 111.
- 12 (a) X.-Q. Lü, W.-X. Feng, Y.-N. Hui, T. Wei, J.-R. Song, S.-S. Zhao, W.-Y. Wong, W.-K. Wong and R. A. Jones, *Eur. J. Inorg. Chem.*, 2010, **18**, 2714; (b) M.-L. Cao, J.-J. Wu, J.-J. Liang and B.-H. Ye, *Cryst. Growth Des.*, 2010, **10**, 4934; (c) G.-F. Zi, F.-R. Zhang, L. Xiang, Y. Chen, W.-H. Fang and H.-B. Song, *Dalton Trans.*, 2010, **39**, 4048; (d) H.-L. Wang, D.-P. Zhang, D.-F. Sun, Y.-T. Chen, K. Wang, Z.-H. Ni, L.-J. Tian and J.-Z. Jiang, *CrystEngComm*, 2010, **12**, 1096; (e) N. Domracheva, A. Pyataev, R. Manapov, M. Gruzdev, U. Chervonova and A. Kolker, *Eur. J. Inorg. Chem.*, 2011, 1291; (f) S.-Q. Su, W. Chen, C. Qin, S.-Y. Song, Z.-Y. Guo, G.-H. Li, X.-Z. Song, M. Zhu, S. Wang, Z.-M. Hao and H.-J. Zhang, *Cryst. Growth Des.*, 2012, **12**, 1808; (g) H.-L. Hsiao, C.-J. Wu, W. Hsu, C.-W. Yeh, M.-Y. Xie, W.-J. Huang and J.-D. Chen, *CrystEngComm*, 2012, **14**, 8143.
- 13 B. Liu, B. Liu, L.-Y. Pang, G.-P. Yang, L. Cui, Y.-Y. Wang and Q.-Z. Shi, *CrystEngComm*, 2013, **15**, 5205.
- 14 (a) J. Wang, Y.-H. Zhang and M.-L. Tong, *Chem. Commun.*, 2006, 3166; (b) J. Wang, S. Hu and M.-L. Tong, *Eur. J. Inorg. Chem.*, 2006, 2069; (c) J. Wang, Z.-J. Lin, Y.-C. Ou, Y. Shen, R. Herchel and M.-L. Tong, *Chem. – Eur. J.*, 2008, **24**, 7218; (d) J. Wang, Y.-C. Ou, Y. Shen, L. Yun, J.-D. Leng, Z.-J. Lin and M.-L. Tong, *Cryst. Growth Des.*, 2009, **9**, 2442.
- 15 (a) A. D. Becke, *J. Chem. Phys.*, 1993, **98**, 1372; (b) C. Lee, W. Yang and R. G. Parr, *Phys. Rev. B: Condens. Matter Mater. Phys.*, 1988, **37**, 785.
- 16 (a) W. J. Hehre, R. Ditchfield and J. A. Pople, *J. Chem. Phys.*, 1972, **56**, 2257; (b) M. J. Frisch, J. A. Pople and J. S. Binkley, *J. Chem. Phys.*, 1984, **80**, 3265.
- 17 M. J. Frisch, *et al.*, *Gaussian 09*, Revision B.01, Inc., Wallingford, CT, 2009.
- 18 G. M. Sheldrick, *SHELXTL97*, program for crystal structure refinement, University of Göttingen, Germany, 1997.
- 19 O. Kahn, *Molecular Magnetism*, VCH Publisher, New York, 1993.
- 20 (a) C.-B. Ma, M.-Q. Hu, H. Chen, M. Wang, C.-X. Zhang, C.-N. Chen and Q.-T. Liu, *CrystEngComm*, 2010, **12**, 1467; (b) L.-F. Ma, M.-L. Han, J.-H. Qin, L.-Y. Wang and M. Du, *Inorg. Chem.*, 2012, **51**, 9431; (c) W.-X. Chen, G.-L. Zhang, L.-S. Long, R.-B. Huang and L.-S. Zheng, *Dalton Trans.*, 2011, **40**, 10237.
- 21 (a) C. M. Nagaraja, R. Haldar, T. K. Maji and C. N. R. Rao, *Cryst. Growth Des.*, 2012, **12**, 975; (b) C. Núñez, R. Bastida, A. Macías, L. Valencia, N. I. Neuman, A. C. Rizzi, C. D. Brondino, P. J. González, J. L. Capelo and C. Lodeiro, *Dalton Trans.*, 2010, **39**, 11654; (c) D. Žilić, B. Rakvin, D. Milić, D. Pajić, I. Dilović, M. Cametti and Z. Džolić, *Dalton Trans.*, 2014, **43**, 11877.
- 22 (a) Z.-J. Lin, B. Xu, T.-F. Liu, M.-N. Cao, J. Lu and R. Cao, *Eur. J. Inorg. Chem.*, 2010, 3842; (b) K. Liu, Y. Peng, F. Yang, D.-X. Ma, G.-H. Li, Z. Shi and S.-H. Feng, *CrystEngComm*, 2014, **16**, 4382.
- 23 (a) S.-Q. Zhang, F.-L. Jiang, M.-Y. Wu, L. Chen, J.-H. Luo and M.-C. Hong, *CrystEngComm*, 2013, **15**, 3992; (b) X. Shi, G.-S. Zhu, Q.-R. Fang, G. Wu, G. Tian, R.-W. Wang, D.-L. Zhang, M. Xue and S.-L. Qiu, *Eur. J. Inorg. Chem.*, 2004, 185.
- 24 (a) F.-L. Liu, L.-L. Zhang, R.-M. Wang, J. Sun, Z. Chen, X.-P. Wang and D.-F. Sun, *CrystEngComm*, 2014, **16**, 2917; (b) J.-Z. Gu, A. M. Kirillov, J. Wu, D.-Y. Lv, Y. Tang and J.-C. Wu, *CrystEngComm*, 2013, **15**, 10287; (c) Y. Zhang, B.-B. Guo, L. Li, S.-F. Liu and G. Li, *Cryst. Growth Des.*, 2013, **13**, 377.
- 25 (a) J. R. Lakowicz, *Principle of Fluorescence Spectroscopy*, Springer, New York, 3rd edn, 2006; (b) M. D. Allendorf, C. A. Bauer, R. K. Bhakta and R. J. T. Houka, *Chem. Soc. Rev.*, 2009, **38**, 1330; (c) J. Zhao, X.-L. Wang, X. Shi, Q.-H. Yang and C. Li, *Inorg. Chem.*, 2011, **50**, 3198; (d) M. Yang, Z.-J. Ouyang, W.-B. Chen, R.-F. Zhou, N. Li and W. Dong, *CrystEngComm*, 2013, **15**, 8529.